ML Symbol Detection for MIMO Systems in the Presence of Channel Estimation Errors

Namsik Yoo[1], Jong-Hyen Back[2], Hyeon-Yeong Choi[2], and Kyungchun Lee[1]
[1] Department of Electrical and Information Engineering, Seoul National University of Science and Technology, 232 Gongneung-ro, Nowon-gu, Seoul, 01811, Republic of Korea
[e-mail: skatlr@seoultech.ac.kr], [e-mail: kclee@seoultech.ac.kr]
[2] Signaling & Communication Team, Metropolitan Transportation Research Center, Korea Railroad Research Institute, 176, Cheldobangmulgwan-ro, Uiwang-si, Gyeonggi-do, 16105, Republic of Korea
[e-mail : jhbaek@krri.re.kr], [e-mail : hchoi@krri.re.kr]
*Corresponding author: Kyungchun Lee

Received February 4, 2016; revised May 30, 2016; revised July 4, 2016; accepted July 31, 2016; published November 30, 2016

Abstract

In wireless communication, the multiple-input multiple-output (MIMO) system is a well-known approach to improve the reliability as well as the data rate. In MIMO systems, channel state information (CSI) is typically required at the receiver to detect transmitted signals; however, in practical systems, the CSI is imperfect and contains errors, which affect the overall system performance. In this paper, we propose a novel maximum likelihood (ML) scheme for MIMO systems that is robust to the CSI errors. We apply an optimization method to estimate an instantaneous covariance matrix of the CSI errors in order to improve the detection performance. Furthermore, we propose the employment of the list sphere decoding (LSD) scheme to reduce the computational complexity, which is capable of efficiently finding a reduced set of the candidate symbol vectors for the computation of the covariance matrix of the CSI errors. An iterative detection scheme is also proposed to further improve the detection performance.

Keywords: MIMO, Maximum Likelihood Detection, List Sphere Decoding, Channel Estimation Error, Channel State Information

A preliminary version of this paper appeared in KICS Summer Conference, June 24-26, 2015, Jeju, Republic of Korea. Compared to the preliminary version, the ILSD scheme, a comparison of computational complexities, and simulation results in various environments are added in this version. This research was supported by a grant from the R&D Program of the Korea Railroad Research Institute, Republic of Korea.

http://dx.doi.org/10.3837/tiis.2016.11.006 **ISSN : 1976-7277**

1. Introduction

In multiple-input multiple-output (MIMO) systems, multiple antennas are employed at the transmitter as well as the receiver. For the same bandwidth and total power, a MIMO system typically provides substantial performance gains in terms of the data rate and reliability with respect to single-antenna systems [1]. Specifically, higher data rates can be achieved by exploiting multiple independent channels between the transmitter and the receiver in order to simultaneously send multiple data streams, whereas a higher reliability can be attained by sending and receiving replicated signals via multiple antennas.

The symbol detection performance significantly affects the overall gains of MIMO systems, and channel state information (CSI) is typically required at the receiver in order to optimally detect symbols. There are various methods to obtain the CSI. As an example, in training-symbol-based estimation, the transmitter sends predetermined symbols, which are exploited for CSI estimation at the receiver [2–4]. In contrast, in blind channel estimation, the covariance matrix of the received signal vectors is exploited to estimate the channel coefficients [5]. Moreover, the importance of training sequence design and subspace-based channel estimation for MIMO systems is addressed in [6], whereas a concept of staggered frame structure for massive MIMO, in which users transmit training pilots at different time, is proposed in [7]. However, regardless of the specific channel estimation method, in practical systems, the estimation performance cannot be perfect, which causes performance degradation in MIMO systems.

There exist many well-known techniques for detecting transmitted symbols, which include the maximum likelihood (ML), zero-forcing (ZF), minimum mean square error (MMSE), and successive interference cancellation (SIC) detection schemes [8, 9]. Among these techniques, the ML detector provides the best performance in terms of the error probability. However, as in the other detection schemes, its detection performance is considerably affected by imperfect CSI. To overcome this problem, a robust ML detector was proposed in [10], which utilizes the CSI error bound. In [11], the variance of the CSI errors is taken into account to improve the performance of the ML detector in the presence of CSI errors. In [12], the optimization of symbol detection by joint processing of the training sequences and data symbols is discussed.

In this paper, a novel ML detection scheme for MIMO systems is proposed. In the proposed iterative ML detection (IMLD) scheme, the instantaneous covariance matrix of the noise and CSI errors is estimated by considering the probabilities of multiple transmit candidate symbol vectors, whereas the published methods [10, 11] use the bound or the long-term statistical information of CSI errors. Then, multiple iterations of the estimation of the covariance matrix and the computation of the symbol probabilities are conducted to improve the error performance. To reduce the computational complexity of the proposed scheme, the iterative list sphere decoding (ILSD) scheme is also proposed, which only exploits a list of selected symbols for the computation of the instantaneous covariance matrix of the noise plus CSI errors.

Notation : Lower-case bold face lettering denotes column vectors. Capital boldface lettering denotes matrices. The symbols $(.)^T$ and $(.)^H$ represent the transpose and conjugate transpose operations, respectively. $\mathbf{I}_N$ denotes an identity matrix with dimensions of $N \times N$.

2. System Model

The numbers of transmit and receive antennas are assumed to be N_t and N_r, respectively. The received signal in the kth symbol interval can be expressed as

$$\mathbf{y}_k = \mathbf{H}\mathbf{x}_k + \mathbf{v}_k, \tag{1}$$

where $\mathbf{x}_k = [x_1, x_1, ..., x_{Nt}]^T$ and $\mathbf{y}_k = [y_1, y_1, ..., y_{Nr}]^T$ denote the transmitted and received signals in the kth symbol interval, respectively, whereas $\mathbf{v}_k = [v_1, v_1, ..., v_{Nr}]^T$ represents the noise signal vector, which is assumed to be a zero-mean complex random vector with a covariance matrix of $\sigma_v^2\mathbf{I}_{N_r}$. Furthermore, $\mathbf{H}$ indicates an $N_r \times N_t$ channel matrix consisting of independent complex Gaussian random elements. An uncorrelated block Rayleigh fading is assumed [13–15]. Specifically, $\mathbf{H}$ is fixed during K symbol intervals, and it is randomly generated every Kth symbol interval.

To consider CSI errors, as in [11, 13], we express the channel matrix $\mathbf{H}$ as $\mathbf{H} = \hat{\mathbf{H}} + \mathbf{E}$, where $\hat{\mathbf{H}}$ is the estimated channel matrix, and $\mathbf{E}$ is a matrix of the CSI errors. It is assumed that $\mathbf{E}$ consists of the instantaneous values of the independent and identically distributed (i.i.d.) random variables having zero mean, which is a widely used assumption for CSI errors in training-symbol-based estimation [2, 3]. Furthermore, $\mathbf{E}$ is assumed to be independent of each $\mathbf{H}$, $\mathbf{x}_k$, and $\mathbf{v}_k$. Then, (1) can be rewritten as

$$\boldsymbol{y}_k = (\hat{\mathbf{H}} + \mathbf{E})\mathbf{x}_k + \mathbf{v}_k = \hat{\mathbf{H}}\mathbf{x}_k + \mathbf{E}\mathbf{x}_k + \mathbf{v}_k = \hat{\mathbf{H}}\mathbf{x}_k + \tilde{\mathbf{v}}_k, \tag{2}$$

where $\tilde{\mathbf{v}}_k = \mathbf{E}\mathbf{x}_k + \mathbf{v}_k$ denotes the effective noise signal that contains the effects of channel estimation errors as well as the additive noise. On the basis of the central limit theorem, for sufficiently large N_t, $\mathbf{E}\mathbf{x}_k$ can be approximately modeled as a Gaussian random vector with zero mean, and the proof for its Gaussianity can be carried out by checking the Lindeberg condition [16], as given in Appendix A.

The covariance matrix of the effective noise, $\tilde{\mathbf{v}}_k$, can be expressed as

$$\begin{aligned}\mathbf{R}_{\tilde{\mathbf{v}}_k} &= \mathbb{E}\left[\tilde{\mathbf{v}}_k\tilde{\mathbf{v}}_k^H\right] = \mathbb{E}[(\mathbf{E}\mathbf{x}_k + \mathbf{v}_k)(\mathbf{E}\mathbf{x}_k + \mathbf{v}_k)^H] \\ &= \sigma_v^2\mathbf{I}_{N_r} + \sigma_x^2\mathbf{E}\mathbf{E}^H,\end{aligned} \tag{3}$$

where $\sigma_x^2 = \mathbb{E}[|x|^2]$ represents the average signal power.

Here, we note that the estimation of $\mathrm{R}_{\tilde{\mathbf{v}}_k}$ is equivalent to the estimation of the covariance matrix of CSI errors, i.e., $\sigma_x^2\mathbf{E}\mathbf{E}^H$, except for the contribution of the noise signal, i.e., $\sigma_v^2\mathbf{I}_{N_r}$.

3. Estimation of the Instantaneous Covariance Matrix

By using the covariance matrix in (3), the ML detection rule in the presence of CSI errors can be expressed as

$$\hat{\mathbf{x}}_k = \arg\max_{\mathbf{x}_k} \frac{1}{\pi^{N_t}\det(\mathbf{R}_{\tilde{\mathbf{v}}_k})} \exp\left\{-\frac{1}{2}(\mathbf{y}_k - \hat{\mathbf{H}}\mathbf{x}_k)^H\mathbf{R}_{\tilde{\mathbf{v}}_k}^{-1}(\mathbf{y}_k - \hat{\mathbf{H}}\mathbf{x}_k)\right\}. \tag{4}$$

The detection of $\mathbf{x}_k$ only depends on the exponential term in (4); hence, the detection rule can be simplified as

$$\hat{\mathbf{x}}_k = \arg\min_{\mathbf{x}_k} \left\{ \left(\mathbf{y}_k - \hat{\mathbf{H}}\mathbf{x}_k\right)^H \mathbf{R}_{\tilde{\mathbf{v}}_k}^{-1} \left(\mathbf{y}_k - \hat{\mathbf{H}}\mathbf{x}_k\right) \right\}. \tag{5}$$

To obtain the solution of (5), knowledge of $\mathbf{R}_{\tilde{\mathbf{v}}_k}$ is required at the receiver. From (2), the effective noise in the *k*th symbol interval can be written as $\tilde{\mathbf{v}}_k = \mathbf{y}_k - \hat{\mathbf{H}}\mathbf{x}_k$, and the instantaneous covariance matrix can be estimated in the form of

$$\mathbf{R}_{\tilde{\mathbf{v}}_k} = \left(\mathbf{y}_k - \hat{\mathbf{H}}\mathbf{x}_k\right)\left(\mathbf{y}_k - \hat{\mathbf{H}}\mathbf{x}_k\right)^H. \tag{6}$$

We note that (6) requires exact knowledge of $\mathbf{x}_k$, which is unavailable at the receiver. Therefore, instead of $\mathbf{x}_k$, we exploit the a-posteriori probabilities of candidate symbol vectors, which can be generated in the detector. The a-posteriori probability of the *i*th candidate symbol vector in the *k*th symbol interval can be written as

$$p_k^i = \frac{1}{P_k \pi^{N_t} \det\left(\hat{\mathbf{R}}_{\tilde{\mathbf{v}},0}\right)} \exp\left\{ -\left(\mathbf{y}_k - \hat{\mathbf{H}}\mathbf{x}_k^i\right)^H \hat{\mathbf{R}}_{\tilde{\mathbf{v}},0}^{-1} \left(\mathbf{y}_k - \hat{\mathbf{H}}\mathbf{x}_k^i\right) \right\}, \tag{7}$$

where $\boldsymbol{x}_k^i$ denotes the *i*th candidate symbol vector in the *k*th symbol interval, and $\hat{\mathbf{R}}_{\tilde{\mathbf{v}},0}$ is the initial estimate of $\mathbf{R}_{\tilde{\mathbf{v}}_k}$. Furthermore, P_k represents the normalization factor that ensures that the sum of all of the probabilities is equal to one, i.e., $\sum_{i=1}^{N_c} p_k^i = 1$. Here, $N_c = 2^{N_t \times N_m}$ is the number of candidate symbol vectors, where N_m is the modulation order. By using (7), $\mathbf{R}_{\tilde{\mathbf{v}}_k}$ can be estimated in the form of

$$\hat{\mathbf{R}}_{\tilde{\mathbf{v}}_k} = \sum_{i=1}^{N_c} p_k^i \left(\mathbf{y}_k - \hat{\mathbf{H}}\mathbf{x}_k^i\right)\left(\mathbf{y}_k - \hat{\mathbf{H}}\mathbf{x}_k^i\right)^H. \tag{8}$$

Under the assumption that the channel matrix and its estimate are fixed for *K* symbol intervals, the covariance matrix of the effective noise can be more accurately estimated by averaging $\hat{\mathbf{R}}_{\tilde{\mathbf{v}}_k}$ for $k = 1, 2, \ldots, K$, i.e.,

$$\mathbf{R}_{\tilde{\mathbf{v}}} = \frac{1}{K} \sum_{k=1}^{K} \hat{\mathbf{R}}_{\tilde{\mathbf{v}}_k}. \tag{9}$$

To compute p_k^i in (7), the initial estimate of $\mathbf{R}_{\tilde{\mathbf{v}}}$ needs to be determined. In (3), the elements of **E** are assumed to be zero-mean i.i.d. random variables, and without any further information, it is reasonable to choose the expectation of $\mathbf{R}_{\tilde{\mathbf{v}}}$ with respect to **E** for its initial estimate:

$$\hat{\mathbf{R}}_{\tilde{\mathbf{v}},0} = (\sigma_v^2 + \sigma_x^2 \sigma_E^2 N_t)\mathbf{I}_{N_r}, \tag{10}$$

where σ_E^2 denotes the variance of each CSI error. Finally, the detector output is generated by substituting $\mathbf{R}_{\tilde{\mathbf{v}}}$ for $\mathbf{R}_{\tilde{\mathbf{v}}_k}$ in (4).

Note that the detection scheme in [11] utilizes (10), which is the expectation of the covariance

matrix, throughout its entire detection process. However, in the proposed algorithms, the covariance matrix is initially set to (10), but it gets updated through multiple iterations so that it approaches its instantaneous value (3), which is capable of providing an improved overall detection performance. The detailed procedures of the proposed algorithms will be described in the subsequent section.

4. Proposed Iterative Algorithms

4.1 Iterative ML Detection (IMLD)

To further improve the performance of the proposed detector, an iterative scheme can be considered. Specifically, the covariance estimate of the effective noise in (8) replaces $\widehat{\mathbf{R}}_{\tilde{\mathbf{v}},0}$ in (7) in the subsequent iteration to update p_k^i, $i = 1, 2, \cdots, N_c$, $k = 1, 2, \cdots, K$. Then, the updated values of p_k^i are used to recalculate $\widehat{\mathbf{R}}_{\tilde{\mathbf{v}}_k}$ and $\mathbf{R}_{\tilde{\mathbf{v}}}$ in (8) and (9). This process is repeated to increase the accuracy of the final detection result. Consequently, the IMLD scheme can be summarized as follows:

- IMLD Algorithm

1. Initialization : Set l = 1 and $\widehat{\mathbf{R}}_{\tilde{\mathbf{v}},0} = (\sigma_v^2 + \sigma_x^2\sigma_E^2 N_t)\mathbf{I}_{N_r}$.
2. Calculate $p_{k,l}^i$, , $i = 1, 2, \cdots, N_c$, $k = 1, 2, \cdots, K$ by using $\widehat{\mathbf{R}}_{\tilde{\mathbf{v}},l-1}$ in (7).
3. Calculate $\widehat{\mathbf{R}}_{\tilde{\mathbf{v}}_k,l}$, $k = 1, 2, \cdots, K$, in (8)
4. Update $\widehat{\mathbf{R}}_{\tilde{\mathbf{v}},l} = \frac{1}{K}\sum_{k=1}^{K} \widehat{\mathbf{R}}_{\tilde{\mathbf{v}}_k,l}$.
5. $l \leftarrow l + 1$.
6. If $l \leq N_{iter}$
   Go to step 2.
   else
   Find the ML solutions $\hat{\mathbf{x}}_k$, $k = 1, 2, \cdots, K$, by using $\widehat{\mathbf{R}}_{\tilde{\mathbf{v}},l}$ in (5).
   end

In this algorithm, l denotes the iteration order. In step 6, if l exceeds the predetermined maximum number of iterations, N_{iter}, the algorithm is terminated by finding the ML solutions.

4.2 Iterative ML Detection (ILSD)

In the previous subsection, we proposed an algorithm that estimates the instantaneous covariance matrix of the effective noise by using the a-posteriori probabilities of all of the candidate symbol vectors. Even though the proposed scheme is capable of providing improved performance, the computational complexity of this estimation increases exponentially with N_m and N_t, rendering the scheme impractical. Hence, we propose to exploit the LSD algorithm, which is capable of reducing computational complexity while achieving near-optimal performance.

LSD is an expansion of the original sphere decoding (SD) scheme. SD is designed to efficiently find a single solution point. Therefore, when a point that is inside the sphere is found, the radius of the sphere for searching the candidate points is updated to the distance between the received signal and the found point [16]. On the other hand, LSD aims to find the

N_L most probable points [17]; hence, LSD fixes the initial radius and selects multiple points that are inside the sphere radius. When the number of selected points is greater than N_L, LSD computes the distance of each selected point from the received signal and selects the N_L points with the smallest distances. In the proposed ILSD scheme, only N_L points, which are selected by LSD, are used to estimate the covariance matrix, $\mathbf{R}_{\tilde{\mathbf{v}}}$, instead of exploiting all of the candidate symbol vectors.

Conventional LSD is typically derived in a real-domain system model [16, 18]. In the rest of this paper, we will employ a real-domain representation for each matrix and vector that can be obtained by using the transformation that is specified in [19]. Then, the cost function in (5) can be represented as

$$\begin{aligned}(\mathbf{y}_k - \hat{\mathbf{H}}\mathbf{x}_k)^T \hat{\mathbf{R}}_{\tilde{\mathbf{v}}}^{-1} (\mathbf{y}_k - \hat{\mathbf{H}}\mathbf{x}_k) &= (\mathbf{x}_k - \check{\mathbf{x}}_k)^T \mathbf{H}^T \hat{\mathbf{R}}_{\tilde{\mathbf{v}}}^{-1} \mathbf{H} (\mathbf{x}_k - \check{\mathbf{x}}_k) \\ &\quad + \mathbf{y}_k^T \left\{ \hat{\mathbf{R}}_{\tilde{\mathbf{v}}}^{-1} - \hat{\mathbf{R}}_{\tilde{\mathbf{v}}}^{-1} \mathbf{H} \left(\mathbf{H}^T \hat{\mathbf{R}}_{\tilde{\mathbf{v}}}^{-1} \mathbf{H} \right)^{-1} \mathbf{H}^T \hat{\mathbf{R}}_{\tilde{\mathbf{v}}}^{-1} \right\} \mathbf{y}_k, \end{aligned} \tag{11}$$

where $\check{\mathbf{x}}_k = \left(\mathbf{H}^T \hat{\mathbf{R}}_{\tilde{\mathbf{v}}}^{-1} \mathbf{H} \right)^{-1} \mathbf{H}^T \hat{\mathbf{R}}_{\tilde{\mathbf{v}}}^{-1} \mathbf{y}_k$. In (11), it is observed that the second term on the right-hand side does not depend on **x**; hence, ML detection can be epressed as

$$\hat{\mathbf{x}}_k = \arg\min_{\mathbf{x}_k} \{ (\mathbf{x}_k - \check{\mathbf{x}}_k)^T \mathbf{U}^T \mathbf{U} (\mathbf{x}_k - \check{\mathbf{x}}_k) \}, \tag{12}$$

where **U** is an $N_t \times N_t$ upper triangular matrix such that $\mathbf{U}^T\mathbf{U} = \mathbf{H}^T \hat{\mathbf{R}}_{\tilde{\mathbf{v}}}^{-1} \mathbf{H}$, and (12) only searches the points that lie inside the sphere with a radius of r, i.e., the points that satisfy $(\mathbf{x}_k - \check{\mathbf{x}}_k)^T \mathbf{U}^T \mathbf{U} (\mathbf{x}_k - \check{\mathbf{x}}_k) \le r^2$. The radius r is determined so that we are reasonably sure that a sufficient number of points exists inside the sphere, as described in [18].

Consequently, the ILSD scheme can be summarized as follows:

- ILSD Algorithm

1. Initialization : Set $l = 1$, $\hat{\mathbf{R}}_{\tilde{\mathbf{v}},0} = (\sigma_v^2 + \sigma_x^2 \sigma_E^2 N_t) \mathbf{I}_{N_r}$, and $\check{\mathbf{x}}_{k,0} = \left(\mathbf{H}^T \hat{\mathbf{R}}_{\tilde{\mathbf{v}},0}^{-1} \mathbf{H} \right)^{-1} \mathbf{H}^T \hat{\mathbf{R}}_{\tilde{\mathbf{v}},0}^{-1} \mathbf{y}_k$.
2. Calculate $\mathbf{U}_{l-1}$ by applying Cholesky factorization to $\mathbf{H}^T \hat{\mathbf{R}}_{\tilde{\mathbf{v}},l-1}^{-1} \mathbf{H}$.
3. Search the points that satisfy $(\mathbf{x}_k - \check{\mathbf{x}}_k)^T \mathbf{U}^T \mathbf{U} (\mathbf{x}_k - \check{\mathbf{x}}_k) \le r^2$, $k = 1, 2, \cdots, K$, to generate a list of N_L points.
4. Calculate $p_{k,l}^i$, , $k = 1, 2, \cdots, K$, for the N_L selected points by using $\hat{\mathbf{R}}_{\tilde{\mathbf{v}},l-1}$ in (7).
5. Calculate $\hat{\mathbf{R}}_{\tilde{\mathbf{v}}_k,l}$, $k = 1, 2, \cdots, K$, in (8).
6. Update $\hat{\mathbf{R}}_{\tilde{\mathbf{v}},l} = \frac{1}{K} \sum_{k=1}^{K} \hat{\mathbf{R}}_{\tilde{\mathbf{v}}_k,l}$ and calculate $\check{\mathbf{x}}_{k,l} = \left(\mathbf{H}^T \hat{\mathbf{R}}_{\tilde{\mathbf{v}},l}^{-1} \mathbf{H} \right)^{-1} \mathbf{H}^T \hat{\mathbf{R}}_{\tilde{\mathbf{v}},l}^{-1} \mathbf{y}_k$.
7. $l \leftarrow l + 1$.
8. If $l \le N_{iter}$
   Go to step 2.
   else
   Select the nearest point to $\check{\mathbf{x}}_{k,l}$ for the ML solution.
   end

In step 3, if the number of selected points is smaller than N_L, the radius increases so that the sphere accommodates a larger number of points. In step 7, if the iteration order is greater than

N_{iter}, the ILSD algorithm is terminated by finding the ML solution. Otherwise, the algorithm returns to step 2 to proceed with the iterations.

5. Computational Complexity

In this section, the computational complexities of the proposed schemes are examined by counting the four fundamental arithmetic operations. To find the inverse of an $N \times N$ matrix, it is assumed that the Gauss-Jordan elimination method is employed, which requires real (complex) operations of $N_3 - N$ additions, $N_3 - N$ multiplications, and $N_2 + N$ divisions for a real (complex) matrix. However, when a matrix is diagonal, N divisions are only required for matrix inversion.

5.1 IMLD

In this subsection, the computational complexity of IMLD is investigated for each step of the algorithm by counting the number of complex operations. In step 1, the algorithm is initialized, and there is no computation. The normalized probabilities are calculated in step 2, where $N_t N_r$ additions and multiplications are needed to calculate $\mathbf{y}_k - \widehat{\mathbf{H}}\mathbf{x}_k^i$, which is stored and utilized in the following iterations. In addition, for the kth symbol interval and N_c symbol candidates, $N_c(N_t + 1)N_r - 1$ additions, $N_c(N_t + 2)N_r$ multiplications and N_c divisions are required in the first iteration ($l = 1$), whereas $N_c N_r^2 - 1$ additions, $N_c(N_r^2 + N_r)$ multiplications, and N_c divisions should be performed in each of the subsequent iterations ($l \neq 1$), where $N_c - 1$ additions and N_c divisions are conducted for the normalization. Furthermore, these computations are repeated for each of the K symbol intervals.

In step 3, $K(N_C - 1)N_r^2$ additions and $2KN_c N_r^2$ multiplications are required during K symbol intervals. The instantaneous covariance matrix is estimated in step 4, which requires $(K - 1)N_r^2$ additions, and N_r^2 divisions. Then, the symbol detection in (5) is performed, where $N_r^3 + KN_c N_r^2 - N_r - KN_c$ additions, $N_r^3 + KN_c N_r^2 + (KN_c - 1)N_r$ multiplications and $N_r^2 + N_r$ divisions are conducted under the assumption that the Gauss-Jordan elimination method is employed for matrix inversion. Consequently, the total computational loads for the K symbol intervals can be summarized as follows:

$$
\begin{aligned}
N_{CA} &= lN_r^3 + \{(l-1)N_t + (l+1)KN_c - l\}N_r^2 - \{(N_r+1)KN_c - l + 2\}N_r \\
&\quad -KN_c - K - l + 1 \ , \\
N_{CM} &= lN_r^3 + 3lKN_c N_r^2 + \{(N_t + l + 2)KN_c - l\}N_r \ , \\
N_{CD} &= (2N_r^2 + N_r + KN_c)l \ ,
\end{aligned}
$$

where N_{CA}, N_{CM}, and N_{CD} denote the numbers of required complex additions, multiplications, and divisions, respectively.

5.2 ILSD

Because a real-domain representation is employed in the ILSD algorithm, real-domain computations are considered for the computational complexity.

In step 1, the estimated solution, $\hat{\mathbf{x}}_k$, is required for the initialization. Hence, $8N_t^3 + (16N_r - 4)N_t^2 + \{4(K-2)N_r - 2(K+1)\}N_t$ additions, $8N_t^3 + 16N_r N_t^2 + \{8N_r^2 +$

$4(K+1)N_r+2\}N_t$ multiplications, and $4N_t^2+2N_t+2N_r$ divisions should be performed during *K* symbol intervals. By assuming $\mathbf{H}^T\widehat{\mathbf{R}}_{\tilde{\mathbf{v}}}^{-1}\mathbf{H}$ is calculated and stored in the previous step, only Cholesky factorization is conducted in step 2, which requires $\frac{8}{3}N_t^3-\frac{2}{3}N_t$ additions, $\frac{8}{3}N_t^3-\frac{2}{3}N_t$ multiplications, and $2N_t-1$ divisions.

In step 3, the bottom-up search algorithm is applied. Because the average number of searched points in each layer varies depending on the amount of noise and channel estimation errors, the computational load of this step is counted and averaged by the simulations, and it is denoted as the subscript "s3." In step 4, the computation of the a-posteriori probability requires $2KN_L(2N_t+1)N_r-K$ additions, $4KN_L(N_t+1)N_r$ multiplications, and KN_L divisions in the first iteration, whereas $4KN_LN_r^2-K$ additions, $KN_L(4N_r^2+2N_r)$ multiplications, and KN_L divisions are required in the subsequent iterations. In step 5, $4K(N_L-1)N_r^2$ additions and $8KN_LN_r^2$ multiplications are performed. Finally, $8N_t^3+(16N_r-4)N_t^2+\{16N_r^2+4(K-6)N_r-K-1\}N_t+8N_r^3+4(K-1)N_r^2-2N_r$ additions, $8N_t^3+16N_rN_t^2+(16N_r^2+4KN_r+2)N_t+8N_r^3-2N_r$ multiplications, and $4N_t^2+2N_t+8N_r^2+2N_r$ divisions are required in step 6. In summary, the total computational complexity for the ILSD scheme during *K* symbol intervals can be expressed as

$$
\begin{aligned}
N_{RA} &= \left(8l+\frac{32}{3}\right)N_t^3+4(l+1)(4N_r-1)N_t^2 \\
&\quad+\left[16lN_r^2+4\{K(l+N_L+1)-2(3l+1)\}N_r-K(l+2)-l-\frac{8}{3}\right]N_t \\
&\quad+8lN_r^3+4K\{lK(N_L+1)-2\}N_r^2-l(2N_r+K)+N_{RA,s3}\,, \\
N_{RM} &= \left(8l+\frac{32}{3}\right)N_t^3+16(l+1)N_rN_t^2 \\
&\quad+\left[8(2l+1)N_r^2+4\{K(l+N_L+1)+1\}N_r+2\left(l+\frac{2}{3}\right)\right]N_t \\
&\quad+8lN_r^3+4(l+1)KN_LN_r^2+2\{(l+1)KN_L-l\}N_r+N_{RM,s3}\,, \\
N_{RD} &= 4(l+1)N_t^2+2(l+2)N_t+8lN_r^2+2(l+1)N_r-1\,,
\end{aligned}
$$

where N_{RA}, N_{RM}, and N_{RD} denote the numbers of real additions, real multiplications, and real divisions, respectively.

6. Simulation Results

6.1 BER Performance

To evaluate the performance of the proposed schemes, computer simulations have been performed. The elements of **H** are assumed to be independent zero-mean complex Gaussian random variables with a unit variance, whereas the elements of the CSI error matrix **E** are independent zero-mean complex Gaussian random variables with a variance of σ_E^2 assuming an uncorrelated block Rayleigh fading channel. It is also assumed that **H** and **E** are constant for *K* symbol intervals.

In the simulation results, the signal-to-noise ratio (SNR) is defined as the ratio of the total average transmit power to the noise variance, i.e.,

$$\mathrm{SNR} = \frac{\sigma_x^2 N_t}{\sigma_v^2}. \tag{13}$$

The performance of the idealized ML and SD detectors with perfect knowledge of the covariance matrix (3) is included for the lower bound of the bit-error-rate (BER) performance, whereas the conventional ML and SD detectors with imperfect CSI represent the upper bound of the BER performance. The robust ML detector in [11] is also considered in the performance comparison. However, the ML detector in [11] does not give any performance gains over the conventional ML detector for constant-modulus modulation schemes in the presence of i.i.d. CSI errors; therefore, its simulation results for QPSK modulation are omitted.

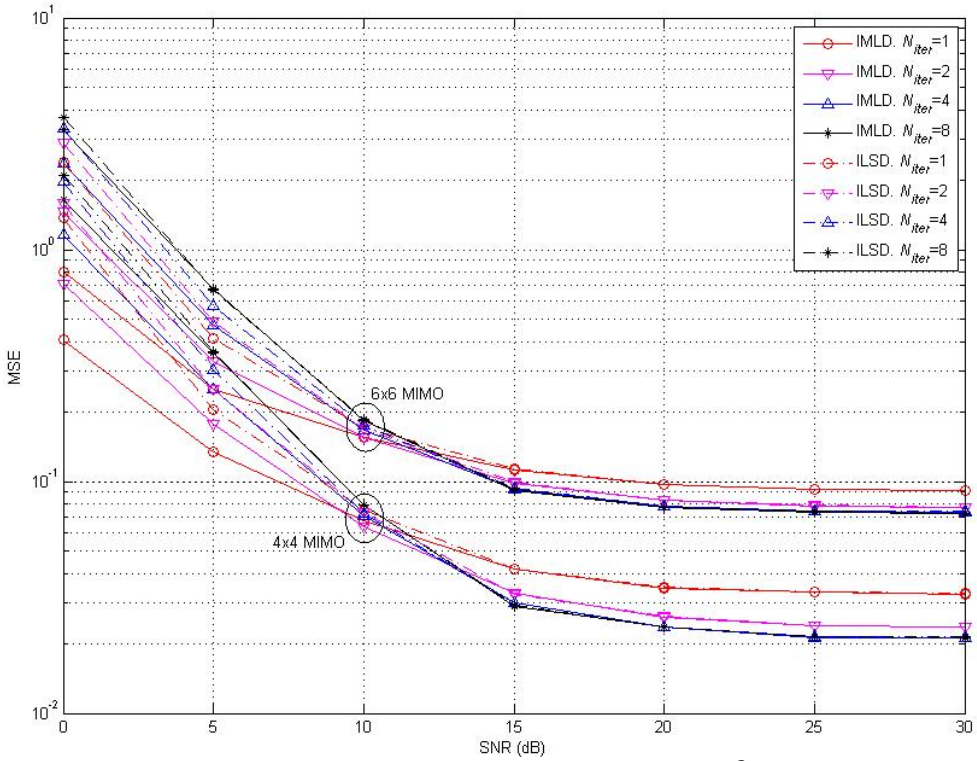

Fig. 1. MSE versus SNR performance : $\mathbf{4 \times 4}$ and $\mathbf{6 \times 6}$ MIMO, QPSK, $\boldsymbol{\sigma_E^2 = -10}$ dB, and K = 32.

To analyze the convergence of the estimated covariance matrix, the mean squared error (MSE) of the estimated covariance matrix is tested, and **Fig. 1** presents the corresponding results for 4×4 and 6×6MIMO systems with $\sigma_E^2 = -10$ dB and K = 32 when QPSK modulation is assumed. In the low SNR region, the MSE increases as the iteration proceeds. This is because incorrect symbol detection results in low SNRs, leading to inaccuracies in the estimation of the covariance matrix. However, in the medium and high SNR regions, it is observed that the MSE decreases as the number of iterations increases, which implies that the potential gains of the proposed detection schemes in terms of the BER are in the medium and high SNR regions. Furthermore, it is seen that there is no significant difference in the MSE between four and eight iterations.

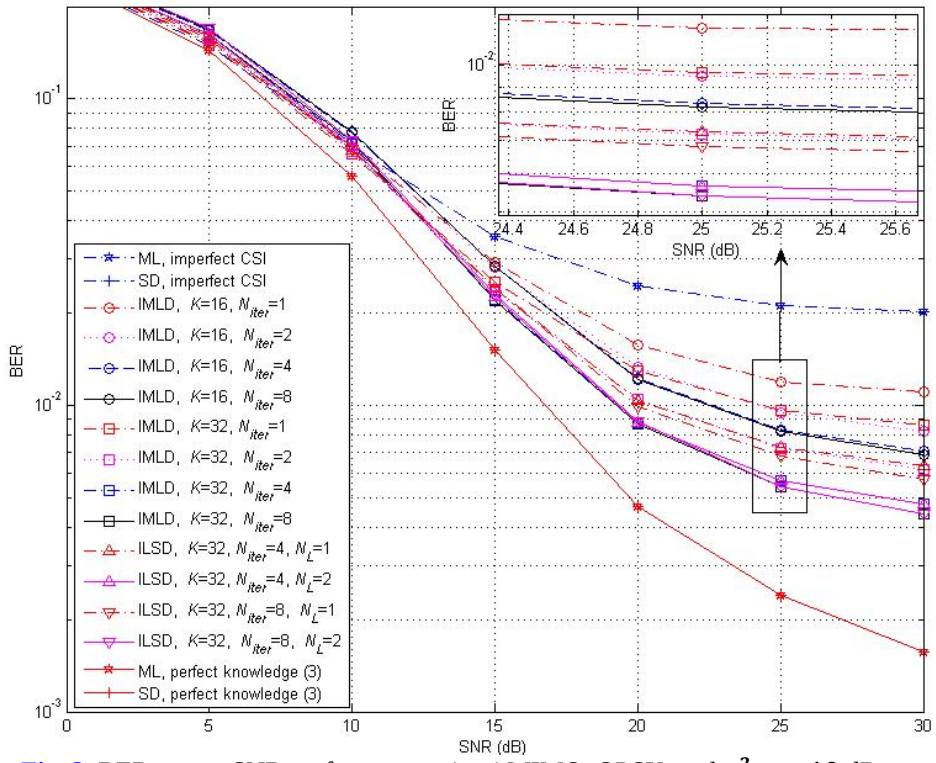

Fig. 2. BER versus SNR performance : 4 × 4 MIMO, QPSK, and $\boldsymbol{\sigma_E^2 = -10}$ dB.

Fig. 2 shows the simulation results of the proposed schemes for a 4 × 4 MIMO system with $\sigma_E^2 = -10$ dB and K = 16, 32 when QPSK modulation is used. In the proposed detection schemes, as K increases, a larger number of received signals are exploited for the estimation of the instantaneous covariance matrix of the effective noise; hence, improved performance is expected. It is observed that the proposed IMLD with K = 16 has an SNR gain of 2.5 dB over the conventional ML scheme with imperfect CSI at a BER of 3×10^{-2}. When the number of symbol intervals is increased to K = 32, this gain is increased to 2.9 dB at the same BER. In addition, compared to the performance in the first iteration, the IMLD scheme with K = 32 achieves SNR gains of 3.8 dB and 5.4 dB at a BER of 10^{-2} after the second and fourth iterations, respectively. However, there is no significant further gain at the same BER after the eighth iteration, which implies that four iterations can be a reasonable choice for the optimal trade-off between the performance and the complexity. On the basis of the simulation results in **Fig. 1** and **2**, the number of iterations will be fixed to four in the forthcoming performance comparisons.

In **Fig. 2**, it is also observed that the ILSD scheme with N_L = 2 provides an SNR gain of 0.8 dB at BER=10^{-2} compared to that with N_L = 1 after the eighth iteration. Furthermore, it is seen that ILSD with N_L = 2 achieves nearly the same performance as IMLD, in spite of its significantly lower computational complexity. Specifically, for the computation of $\widehat{\mathbf{R}}_{\tilde{\mathbf{v}}}$ in the corresponding simulation environment, ILSD with N_L = 2 only takes two selected candidate solution vectors into account in each symbol interval, whereas IMLD needs to consider $2^{N_t \times N_m} = 2^{16}$ solution vectors.

In the derivation of the proposed detection schemes, it is claimed that the effect of CSI errors, $\mathbf{Ex}_k$, can be approximately modeled as Gaussian random variables under the assumption that N_t is sufficiently large, and its proof is given in Appendix A. However, in **Fig. 2**, it is seen that, even for N_t = 4, the IMLD scheme achieves substantial gains over the conventional ML detector in the presence of CSI errors by taking the covariance matrix of the effective noise into account.

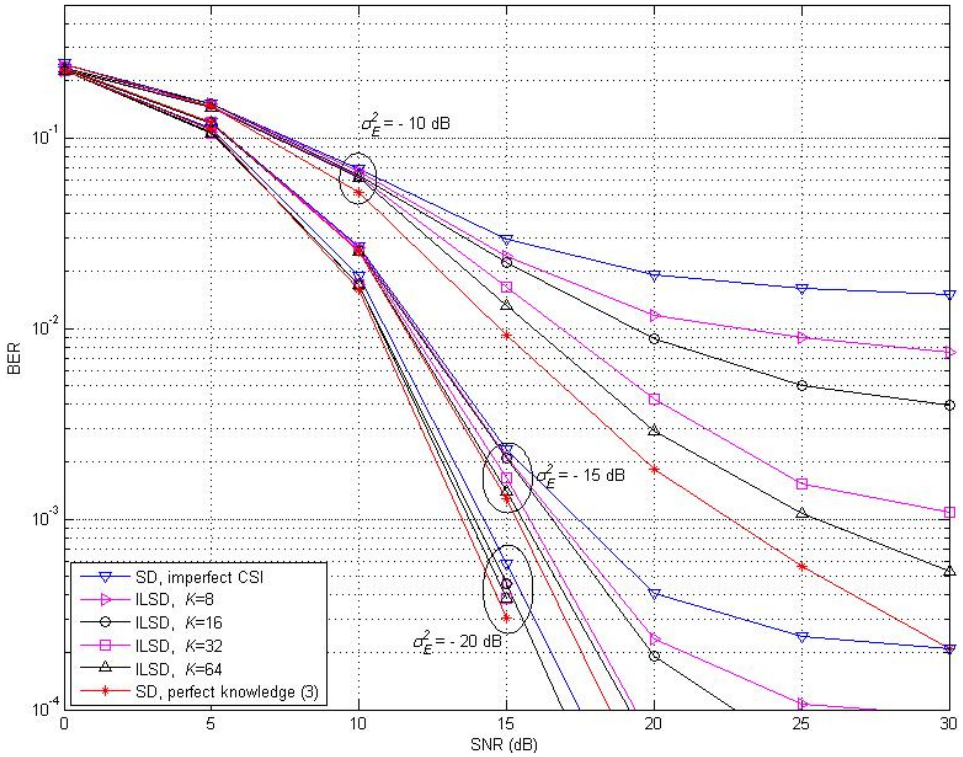

Fig. 3. BER versus SNR performance : 6 × 6 MIMO, QPSK, $\boldsymbol{N_L = 2}$, and $\boldsymbol{N_{iter} = 4}$.

Fig. 3 shows the BER performance of the ILSD scheme and conventional SD for a 6 × 6 MIMO system with various values of σ_E^2 when QPSK modulation is used. For σ_E^2= −20 dB, the ILSD scheme achieves nearly the same performance as the idealized SD with perfect knowledge of the covariance matrix. It is also seen that the ILSD scheme with K = 32 only has a marginal performance degradation with respect to idealized SD for σ_E^2 = −15 dB. Furthermore, it is seen that the proposed ILSD scheme provides significant SNR gains over conventional SD, which proves its robustness to CSI errors. In particular, for σ_E^2 = −10 dB, the ILSD schemes with K = 16, K = 32, and K = 64 achieve 4.1 dB, 5.2 dB, and 5.7 dB SNR gains respectively, over conventional SD at a BER of 2×10^{-2}.

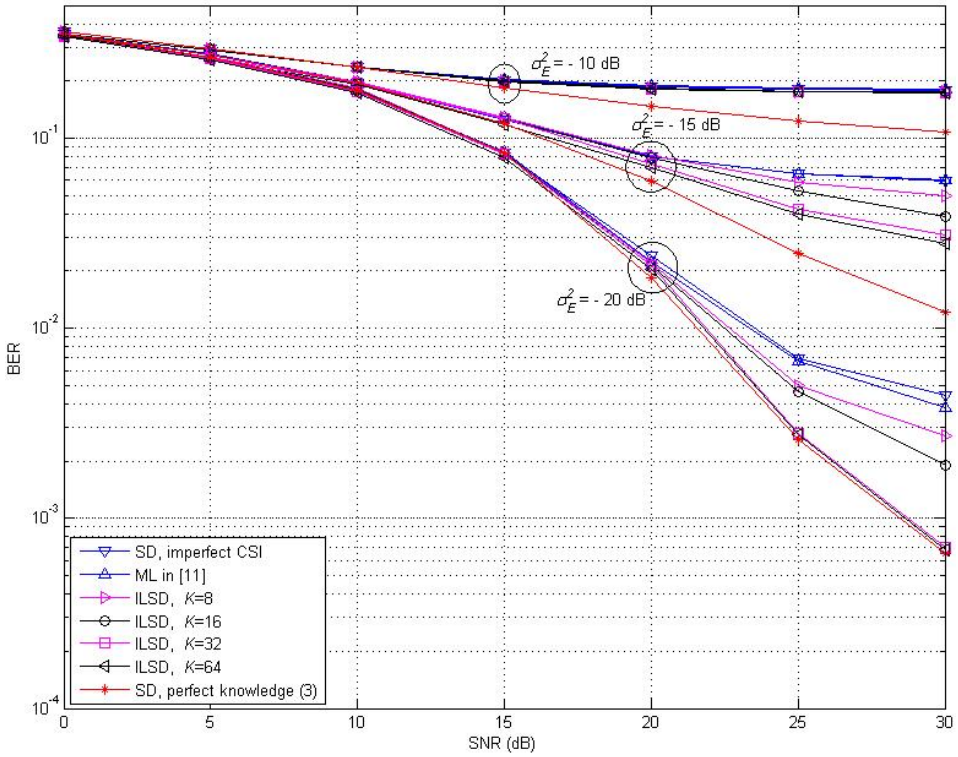

Fig. 4. BER versus SNR Performance : 4×4 MIMO, 16QAM, $\boldsymbol{N_L = 2}$, and $\boldsymbol{N_{iter} = 4}$.

Fig. 4 presents the BER performance of the proposed scheme and robust ML in [11] for 4×4 MIMO when 16-QAM modulation is assumed. The ILSD scheme with K = 16 exhibits an SNR gain of 1.4 dB at BER=10^{-2} over robust ML in [11] for σ_E^2 = −20 dB, and this gain increases to 2.2 dB when K is doubled at the same BER. These performance gains result from the fact that the proposed schemes estimate the instantaneous covariance matrices of CSI errors for ML symbol detection, which provide improved robustness against CSI errors, whereas the algorithm in [11] only utilizes the long-term statistical information of CSI errors.

6.2 Complexity Comparison

In this subsection, the computational complexities of the proposed schemes and conventional ML and SD are investigated by using the results in Section 5. For a proper comparison, the complexity in the complex domain is converted to that in the real domain, which can be summarized as follows:

$$N_{CA} = 2N_{RA}\,,$$
$$N_{CM} = 2N_{RA} + 4N_{RM}\,,$$
$$N_{CD} = 4N_{RA} + 6N_{RM} + 2N_{RD}\,.$$

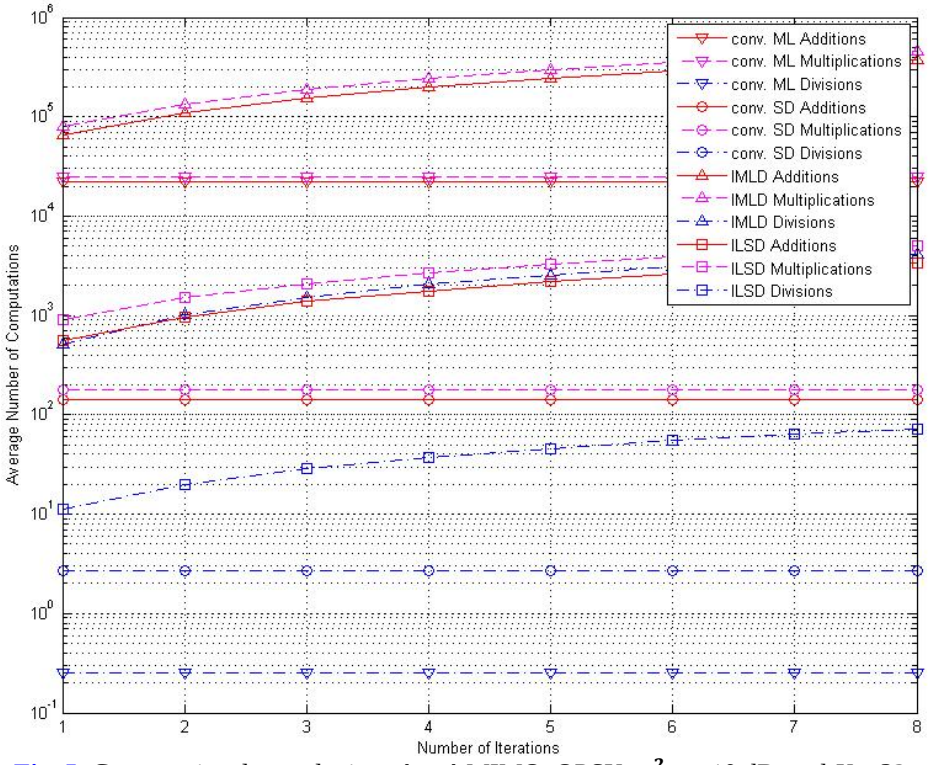

Fig. 5. Computational complexity : $\mathbf{4} \times \mathbf{4}$ MIMO, QPSK, $\boldsymbol{\sigma_E^2}$ = −10 dB, and K = 32.

Fig. 5 shows the average number of real arithmetic operations for 4 × 4 MIMO, $\sigma_E^2 = -10$dB, K = 32, and the QPSK modulation. As the number of iterations increase, the computational complexities of the proposed iterative detection schemes also increase, whereas the conventional non-iterative schemes require a fixed amount of computational load. In Fig. 5, it is seen that the ILSD scheme requires a higher number of operations compared to the conventional SD scheme. The number of operations is approximately 4.9 times, 8.5 times, and 15.1 times larger after the first, second, and fourth iterations, respectively. Similarly, for real additions, the ILSD scheme requires 3.9 times, 6.8 times, and 12.5 times higher complexity than the conventional SD scheme after the first, second, and fourth iterations, respectively. However, it is found that the ILSD scheme attains a significant reduction in the computational load with respect to the IMLD scheme. Specifically, the ILSD scheme only requires 0.9 % of additions, 1.1 % of multiplications, and 1.8 % of divisions compared to the IMLD scheme; however, nearly the same BER performance is achieved, as shown in **Fig. 2**.

7. Conclusion

In this paper, we have proposed novel iterative ML detection algorithms for MIMO systems that are robust to CSI errors. The proposed schemes estimate the instantaneous covariance matrix of the effective noise, which contains the effects of CSI errors as well as the additive noise. In the proposed IMLD scheme, the a-posteriori probabilities of all of the candidate solution points are considered to estimate the instantaneous covariance matrix of the effective noise. In contrast, in the ILSD scheme, it is only estimated by exploiting a list of the selected points that lie inside a sphere. Despite its substantially lower complexity, the simulation

results show that ILSD with $N_L = 2$ nearly achieves the BER performance of IMLD. To further improve the performance of the proposed detection schemes, the covariance matrix of the effective noise is iteratively estimated on the basis of the updated probabilities of the candidate solution points.

In the simulation results, it is shown that the IMLD and ILSD schemes provide significant performance gains over the conventional ML detector in the presence of channel estimation errors, especially in medium and high SNR regions, which are typical operating SNR regions for mobile communication systems. Specifically, for a 6 × 6 MIMO system with $\sigma_E^2 = -15$ dB, $K = 32$, and QPSK modulation, ILSD provides an SNR gain of 3.4 dB at BER=4×10^{-4} over the conventional ML detector. The computational complexity is also evaluated, which shows that ILSD achieves a significant reduction of the computational complexity compared to IMLD.

For future work, the extension of the proposed detection algorithm to soft decoding for coded MIMO systems can be considered.

Appendix A: Proof for the Gaussianity of Ex

The *m*th element of **Ex** can be written as

$$[\mathbf{Ex}]_m = \sum_{n=1}^{N_t} \delta_{mn} x_n \,, \tag{A.1}$$

where $[\cdot]_m$ denotes the *m*th element of a vector, and δ_{mn} represents the element at the *m*th row and *n*th column of **E**. We assume that δ_{mn} for $m = 1, 2, \cdots, N_r$ and $n = 1, 2, \cdots, N_t$, represents the instantaneous values of i.i.d. random variables. We denote the normalized real part of $[\mathbf{Ex}]_m$ as

$$z_m = s_{N_t}^{-1} \sum_{n=1}^{N_t} \left\{ \delta_{mn,R} x_{n,R} - \delta_{mn,I} x_{n,I} \right\} , \tag{A.2}$$

where

$$s_{N_t}^{-1} = \sum_{n=1}^{N_t} \frac{\sigma_x^2}{2} \left\{ \delta_{mn,R}^2 + \delta_{mn,I}^2 \right\} , \tag{A.3}$$

and the subscripts *R* and *I* represent the real and imaginary parts of a complex number, respectively. Then, for a given set of instantaneous values of δ_{mn}, we will prove that z_m converges to a standard Gaussian random variable as $N_t \to \infty$ when the transmitted signals $x_{n,R}$ and $x_{n,I}$ are considered as i.i.d. zero-mean random variables.

In (A. 2), z_m can be observed as the sum of independent random variables $\delta_{mn,R} x_{n,R}$ and $\delta_{mn,I} x_{n,I}$, $n = 1, 2, \cdots, N_t$. We note that they are not identically distributed owing to different instantaneous values of $\delta_{mn,R}$ and $\delta_{mn,I}$. In order to check if z_m converges to a standard Gaussian distribution, we test the Lindeberg condition [16]. For the signal model in (A. 2), the Lindeberg condition can be reformulated as

$$\frac{1}{s_{N_t}^2}\sum_{n=1}^{N_t}\left\{\delta_{mn,R}^2\mathbb{E}\left[x_{n,R}^2 I\left(|x_{n,R}|>\frac{\eta s_N}{\delta_{mn,R}}\right)\right]+\delta_{mn,I}^2\mathbb{E}\left[x_{n,I}^2 I\left(|x_{n,R}|>\frac{\eta s_N}{\delta_{mn,I}}\right)\right]\right\}\to 0$$
$$\text{as } \mathrm{N_t}\to\infty, \forall\eta>0\,, \quad (A.4)$$

where $I(.)$ is the indicator function

$$I(A)=\begin{cases}1 & \text{if A is true,}\\ 0 & \text{if A is false.}\end{cases} \quad (A.5)$$

We define $\delta_{m,max}$ as the maximum value among $\{\delta_{m1,R},\ \cdots,\delta_{mN_t,R},\delta_{m1,I},\ \cdots,\delta_{mN_t,I}\}$. Then, the left-hand side of (A.4) satisfies the following inequality:

$$\begin{aligned}
&\frac{1}{s_{N_t}^2}\sum_{n=1}^{N_t}\left\{\delta_{mn,R}^2\mathbb{E}\left[x_{n,R}^2 I\left(|x_{n,R}|>\frac{\eta s_N}{\delta_{mn,R}}\right)\right]+\delta_{mn,I}^2\mathbb{E}\left[x_{n,I}^2 I\left(|x_{n,R}|>\frac{\eta s_N}{\delta_{mn,I}}\right)\right]\right\}\\
&\le\frac{1}{s_{N_t}^2}\sum_{n=1}^{N_t}\left\{\delta_{mn,R}^2\mathbb{E}\left[x_{n,R}^2 I\left(|x_{n,R}|>\frac{\eta s_N}{\delta_{m,max}}\right)\right]+\delta_{mn,I}^2\mathbb{E}\left[x_{n,I}^2 I\left(|x_{n,R}|>\frac{\eta s_N}{\delta_{m,max}}\right)\right]\right\}\\
&=\frac{1}{s_{N_t}^2}\sum_{n=1}^{N_t}\left(\delta_{mn,R}^2+\delta_{mn,I}^2\right)\mathbb{E}\left[x_{1,R}^2 I\left(|x_{1,R}|>\frac{\eta s_N}{\delta_{m,max}}\right)\right]\\
&=\frac{2}{\sigma_x^2}\mathbb{E}\left[x_{1,R}^2 I\left(|x_{1,R}|>\frac{\eta s_N}{\delta_{m,max}}\right)\right]. \quad (A.6)
\end{aligned}$$

The third line of (A.6) is obtained from the fact that $x_{n,R}$ and $x_{n,I}$ are i.i.d. random variables. A sufficient condition for (A.6) to converge to zero can be expressed as

$$\frac{s_{N_t}}{\delta_{m,max}}\to\infty \text{ as } N_t\to\infty\,. \quad (A.7)$$

In (A.3), $s_{N_t}^2$ is the sum of $2N_t$ instantaneous values of the i.i.d. random variables $\delta_{mn,R}^2$ and $\delta_{mn,I}^2$, which have positive mean values. Hence, we have $s_{N_t}\to\infty$ as $N_t\to\infty$, which implies (A.7). Consequently, (A.6) converges to zero, which proves that Lindeberg condition of (A.4) is satisfied.

For the normalized imaginary part of $[\mathbf{Ex}]_m$, similar steps can be performed to prove that it also tends to a standard Gaussian random variables; therefore, it is concluded that $[\mathbf{Ex}]_m$ can be approximated as a complex Gaussian random variable for sufficiently large N_t.

References

[1] L. Zheng and D. N. C. Tse, "Diversity and multiplexing: A fundamental tradeoff in multiple-antenna channels," *IEEE Transactions on Information Theory*, vol.49, no.5, pp.1073–1096, 2003. Article (CrossRef Link)

[2] B. Hassibi and B. M. Hochwald, "How much training is needed in multiple-antenna wireless links?" *IEEE Transactions on Information Theory*, vol.49, no.4, pp.951–963, 2003. Article (CrossRef Link)

[3] T. L. Marzetta, "BLAST training: estimating channel characteristics for high-capacity space-time wireless," in *Proc. of 37th Annual Allerton Conference Communications, Control, and Computing*, vol. 37, pp. 958-966, 1999. Article (CrossRef Link)
[4] M. Biguesh and A. B. Gershman, "Training-based MIMO channel estimation: A study of estimator tradeoffs and optimal training signals," *IEEE Transactions on Signal Processing*, vol.54, no.3, pp.884–893, 2006. Article (CrossRef Link)
[5] S. Shahbazpanahi, A. B. Gershman, and J. H.Manton, "Closed-form blind MIMO channel estimation for orthogonal space-time block codes," *IEEE Transactions on Signal Processing*, vol.53, no.12, pp.4506–4517, 2005. Article (CrossRef Link)
[6] D. Qu, G. Zhu, and T. Jiang, "Training Sequence Design and Parameter Estimation of MIMO Channels with Carrier Frequency Offsets," *IEEE Transactions on Wireless Communications*, vol.5, no.12, pp.3662-3666, Dec. 2006. Article (CrossRef Link)
[7] D. Kong, D. Qu, K. Luo, and T. Jiang, "Channel Estimation under Staggered Frame Structure for Massive MIMO system," *IEEE Transactions on Wireless Communications*, vol.15, no.2, pp.1469-1479, 2016. Article (CrossRef Link)
[8] J. L. Melsa and D. L. Cohn, *Decision and Estimation Theory*, McGraw-Hill, 1978.
[9] V. Trees and Harry L, *Detection, Estimation, and Modulation theory*, John Wiley & Sons, 2004.
[10] A. A. Farhoodi and M. Biguesh, "Robust ML detection algorithm for MIMO receivers in presence of channel estimation error," in *Proc. of 2006 IEEE 17th International Symposium on Personal, Indoor and Mobile Radio Communications*, pp.1–5, 2006. Article (CrossRef Link)
[11] B. S. Thian and A. Goldsmith, "Reduced-complexity robust MIMO decoders," *IEEE Transactions on Wireless Communications*, vol.12, no.8, pp.3783–3795, 2013. Article (CrossRef Link)
[12] G. Taricco and E. Biglieri, "Space-time decoding with imperfect channel estimation," *IEEE Transactions on Wireless Communications*, vol.4, no.4, pp.1874–1888, 2005. Article (CrossRef Link)
[13] Z. Zhou and B. Vucetic, "Design of adaptive modulation using imperfect CSI in MIMO systems," *Electronics Letters*, vol.40, no.17, pp.1073–1075, 2004. Article (CrossRef Link)
[14] R.-R. Chen, R. Koetter, U. Madhow, and D. Agrawal, "Joint noncoherent demodulation and decoding for block fading channel: A practical framework for approaching Shannon capacity," *IEEE Transactions on Communication*, vol. 51, no. 10, pp. 1676-1689, Oct. 2003. Article (CrossRef Link)
[15] M.M´edard and D. N. C. Tse, "Spreading in block-fading channels," in *Proc. 34th Asilomar Conference on Signals, Systems and Computers*, vol.2, pp.1598-1602, Oct. 2000. Article (CrossRef Link)
[16] S. I. Resnick, *A Probability Path*, Springer Science & Business Media, 2013.
[17] B. Hassibi and H. Vikalo, "On the sphere-decoding algorithm I. Expected complexity," *IEEE Transactions on Signal Processing*, vol.53, no.8, pp.2806–2818, 2005. Article (CrossRef Link)
[18] B. M. Hochwald and S. ten Brink, "Achieving near-capacity on a multiple-antenna channel," *IEEE Transactions on Communications*, vol.51, no.3, pp.389–399, 2003. Article (CrossRef Link)
[19] J. Jald´en and B. Ottersten, "On the complexity of sphere decoding in digital communications," *IEEE Transactions on Signal Processing*, vol.53, no.4, pp.1474–1484, 2005. Article (CrossRef Link)

Namsik Yoo received B.S. and M.S. degrees in electrical and information engineering from Seoul National University of Science and Technology, Korea, in 2013 and 2016, respectively. His main research interests are signal processing and detection/estimation techniques for massive MIMO.

Jong-Hyen BACK received the B.S. degrees in electronic control engineering in 1995, respectively from CHONBUK University, Korea. He also received the M.S. degrees in mechatronics engineering in 1997, respectively from Kwang-Ju Institute of Science and Technology, and the Ph.D. degrees in Mechatronics engineering from CHONBUK University, Korea. Since 1997, he has served as a researcher in Korea Railroad Research Institute (KRRI). His research interests include train control system, automatic train control & protection.

Hyeon-Yeong CHOI received the B.S. degree in electrical engineering from University of Seoul, Seoul, South Korea, in 2003, and the M.S. and Ph.D. degrees in electrical engineering from Korea Advanced Institute of Science and Technology (KAIST), Daejeon, South Korea, in 2005 and 2010, respectively. From 2011 to 2013, she was a research engineer at KDDI R&D Laboratories Inc., Japan, where she was engaged in research and development of photonic transport networks and future optical networks. She is currently with Korea Railroad Research Institute (KRRI), South Korea. Her research interests include integrated wireless network for railway and intelligent train control system.

Kyungchun Lee received B.S., M.S., and Ph.D. degrees in electrical engineering from Korea Advanced Institute of Science and Technology (KAIST), Daejeon, in 2000, 2002, and 2007, respectively. From April 2007 until June 2008, he held a postdoctoral research fellowship at the University of Southampton, United Kingdom. From July 2008 to August 2010, he was with Samsung Electronics, Suwon, Korea. Since September 2010, he has been with Seoul National University of Science and Technology, Korea. He received the Best Paper Award at the IEEE International Conference on Communications in 2009. His research interests include signal processing and optimization for wireless communications with a focus on massive MIMO, interference coordination, and cooperative systems.